Progress In Electromagnetics Research, PIER 91, 393–411, 2009

AN UNEQUAL DUAL-FREQUENCY WILKINSON POWER DIVIDER WITH OPTIONAL ISOLATION STRUCTURE

Y. Wu, Y. Liu, and S. Li

School of Electronic Engineering
Beijing University of Posts and Telecommunications
Beijing, China

Abstract—In this paper, we propose a generalized Wilkinson power divider operating at two arbitrary frequencies with unequal power dividing ratio. To achieve unequal power division and perfect matching at dual-frequency, a novel structure consisted of four dual-frequency transformers in two sections is proposed. For the compact power divider, the parallel and series RLC structures can be chosen to obtain effective isolation between the two outports according to different frequency ratios. Furthermore, the closed-form design equations of the unequal dual-frequency power divider are derived based on circuit theory and transmission line theory. Finally, simulation and experiment results of two examples including parallel and series RLC structures indicate that all the theoretical features of these unequal power dividers can be fulfilled at dual-frequency simultaneously.

1. INTRODUCTION

Design of dual band (dual-frequency) components such as antennas [1, 2], filters [3], and transformers [4–7] is the research focus. As the key components, power dividers are widely used in microwave and millimeter-wave systems. In usual, the conventional power dividers are designed at a single band [8–11]. Recently, many researches have been made in designing new Wilkinson power dividers for dual-frequency application [12–20]. In obtaining ideal isolation effect in various dual-frequency power dividers, three novel isolation structures including parallel RLC [13], series RLC [14], and combining of parallel R and series LC [15] demonstrate better isolating effect than traditional single resistor isolators on the same layouts. In [16–20], other modified types

Corresponding author: Y. Wu (wuyongle138@gmail.com).

of Wilkinson power dividers without reactive components have been proposed to operate at dual band. In order to break the limit of equal output power at the two outports of these dual band power dividers in [12–20], dual band power dividers with unequal power dividing have been proposed in [21] and [22], however, the design parameters cannot be obtained using analytical approach [21] while the perfect matching of outports in the corresponding design procedure are not theoretically considered [22]. Furthermore, to obtain the perfect matching at all of ports and isolation between the two outports, a new unequal Wilkinson power divider for a frequency and its first harmonic has been proposed in [23]. Although the design method is analytical, the coefficient of the frequency ratio (which must equal to 2) is constant. In addition, the other new kinds of dual band unequal power divider with flexible dual-frequency ratios (which is not limited) have been presented in [24–27] as extensions of the previous equal dual band power dividers. In order to obtain high and general characteristics of power dividers, new structures of unequal dual band power dividers with closed-form design equations and wide available frequency-ratio range need to be researched further.

In this paper, we propose a new structure of ***unequal*** Wilkinson power divider operating at two ***arbitrary*** frequencies with ***wide*** available frequency-ratio range and ***optional*** isolation structure. Since the impedance characteristics are asymmetric, the traditional even-mode and odd-mode methods unsuitable for unequal cases are not applicable. Instead, we adopt the analysis methods [23] of the ideal transmission line theory and circuit theory in this paper. Based on these methods, the analytical design solutions for this novel generalized power divider are then obtained. In addition, to assure that the values of reactive components (L and C) as the isolation structure are positive and the total structure is compact, an important rule to choose isolation structure according to the desired frequency ratios is summarized as follows (namely, optional isolation structure): (i) when the frequency ratio is lesser than 3, the parallel RLC is chosen; (ii) When the frequency ratio equals to 3, only the resistor R should be chosen, which is actually the same with the conventional unequal Wilkinson power divider [8]; (iii) when the frequency ratio is greater than 3, the series RLC is chosen. Obviously, this proposed power divider, to a large extent, is a more generalized model of traditional power divider. In other words, the preceding dual-frequency equal Wilkinson power divider [13] and conventional unequal Wilkinson power divider [8] are special cases of this proposed power divider.

2. THEORY AND DESIGN EQUATIONS

In this section, the circuit model of our proposed unequal dual-frequency Wilkinson power divider is given, and analysis and parameters design are based on it. Figure 1 schematically shows the circuit model of our proposed structure. Four small dual-frequency transformers in two sections [4] are impedance matched at the two arbitrary center frequencies. The characteristic impedances of different sections with different subscripts are asymmetric in order to achieve unequal power dividing ratio. The isolation effect of the divider is improved by the introduction of an isolator Z, whose circuit structure will be discussed in Subsection 2.3.

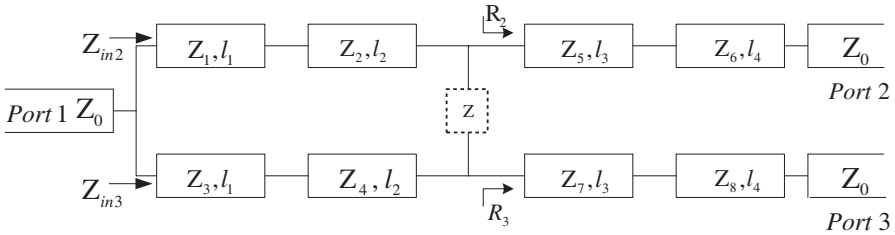

Figure 1. Proposed circuit model of unequal dual-frequency power divider.

2.1. Characteristic Impedances Design

In order to achieve the desired power dividing ratio $P_3/P_2 = k^2$, the input impedances in Figure 1 should be [23],

$$R_2 = k^2 R_3, \qquad Z_{in\,2} = k^2 Z_{in\,3}. \tag{1}$$

Also, to meet the matching conditions at port 1 (characteristic impedance equals Z_0), the relationship of the input impedances should be expressed as,

$$Z_0 = \frac{Z_{in\,2} Z_{in\,3}}{Z_{in\,2} + Z_{in\,3}} = \frac{k^2}{1+k^2} Z_{in\,3}. \tag{2}$$

Combining (1) and (2), the two input impedances can be written as

$$Z_{in\,2} = (1+k^2) Z_0, \quad Z_{in\,3} = \frac{1+k^2}{k^2} Z_0. \tag{3}$$

Usually, R_2 and R_3 can be defined as,

$$R_2 = kZ_0, \qquad R_3 = \frac{Z_0}{k}. \tag{4}$$

Based on Monzon's theory [4], for impedance matching of each port at both frequencies f_1 and $f_2 = uf_1$, $u \geq 1$, or correspondingly with phase constants β_1 and $\beta_2 = u\beta_1$ (where u is the frequency ratio), the characteristic impedances of all sections must satisfy the following expressions:

$$Z_1 = Z_0(k^2+1)\sqrt{\frac{2p^2k}{H}}, \quad Z_2 = Z_0\sqrt{\frac{kH}{2p^2}}, \tag{5}$$

$$Z_3 = Z_0\frac{(k^2+1)}{k^2}\sqrt{\frac{2p^2k}{H}}, \quad Z_4 = \frac{Z_0}{k^2}\sqrt{\frac{kH}{2p^2}}, \tag{6}$$

$$Z_5 = Z_0\sqrt{\frac{k}{2p^2}(1-k) + \sqrt{\left[\frac{k}{2p^2}(1-k)\right]^2 + k^3}}, \quad Z_6 = \frac{kZ_0^2}{Z_5}, \tag{7}$$

$$Z_7 = \frac{Z_6}{k}, \quad Z_8 = \frac{Z_5}{k}, \tag{8}$$

where

$$H = \left[k^2 + 1 - k + \sqrt{(k-k^2-1)^2 + 4p^4k(k^2+1)}\right], \tag{9}$$

$$p = \tan\left(\frac{n\pi}{1+u}\right). \tag{10}$$

And the corresponding physical lengths in Figure 1 are

$$l = l_1 = l_2 = l_3 = l_4 = \frac{n\lambda_1}{2(1+u)}, \quad n \in N^+, \tag{11}$$

where λ_1 is the wavelength of the frequency f_1 and N^+ are positive integers.

However, in this paper we only discuss the compact structure with the shortest physical length when $n = 1$. On the one hand, compactness is always an important goal pursued by industrial applications. On the other hand, the compact structure is also the most extreme case and its physical implementation guarantees the implementation of other less compact structures when $n > 1$, because they realize the same function as the compact structure. Substituting

$n = 1$ into (10) and (11) and we get

$$l = l_1 = l_2 = l_3 = l_4 = \frac{\lambda_1}{2(1+u)}, \tag{12}$$

and

$$p = \tan\left(\frac{\pi}{1+u}\right). \tag{13}$$

All the following discussions are based on (12) and (13).

2.2. Parameters Solutions of Isolation Structure

To determine the parameters of isolation structure Z in Figure 1, it is necessary to employ a combined analysis with both circuit theory and transmission line theory [23, 24]. By replacing the matched transmission lines at the outports with the equivalent loads and linking a voltage source V_S to port 2, the voltages and currents can be defined directly, as illustrated in Figure 2.

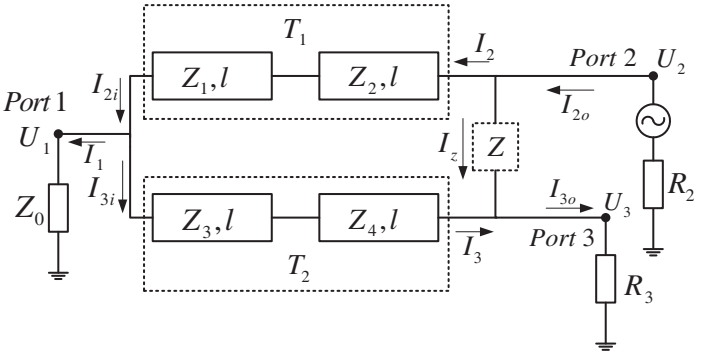

Figure 2. Equivalent circuit of the proposed power divider with voltage generator at outport 2.

According to Kirchhoff's laws in circuit theory, the relation between currents and voltages can be expressed as

$$\begin{aligned} &U_1 = I_1 Z_0, \quad I_{2i} = I_1 + I_{3i}, \quad I_{2o} = I_2 + I_z, \\ &I_z = \frac{U_2 - U_3}{Z}, \quad I_{3o} = I_3 + I_z, \quad I_{3o} = \frac{U_3}{R_3}. \end{aligned} \tag{14}$$

In the transmission line theory, the currents and voltages on transmission lines can also be analytically correlated by the

transmission matrices

$$T_1 = \begin{bmatrix} A_{T1} & B_{T1} \\ C_{T1} & D_{T1} \end{bmatrix} = \begin{bmatrix} \cos^2(\beta l) - (Z_2/Z_1)\sin^2(\beta l) & 0.5j\sin(2\beta l)(Z_1+Z_2) \\ 0.5j\sin(2\beta l)/(Z_1+Z_2) & \cos^2(\beta l) - (Z_1/Z_2)\sin^2(\beta l) \end{bmatrix}, \quad (15)$$

$$T_2 = \begin{bmatrix} A_{T2} & B_{T2} \\ C_{T2} & D_{T2} \end{bmatrix} = \begin{bmatrix} \cos^2(\beta l) - (Z_3/Z_4)\sin^2(\beta l) & 0.5j\sin(2\beta l)(Z_3+Z_4) \\ 0.5j\sin(2\beta l)/(Z_3+Z_4) & \cos^2(\beta l) - (Z_4/Z_3)\sin^2(\beta l) \end{bmatrix}. \quad (16)$$

And then, the relationship between the corresponding currents and voltages can be expressed as

$$\begin{cases} U_2 = A_{T1}U_1 + B_{T1}I_{2i} \\ I_2 = C_{T1}U_1 + D_{T1}I_{2i} \\ U_1 = A_{T2}U_3 + B_{T2}I_3 \\ I_{3i} = C_{T2}U_3 + D_{T2}I_3 \end{cases}. \quad (17)$$

To achieve ideal isolating effect, U_3 must be zero. That is

$$U_3 = 0. \quad (18)$$

From (14)–(17), we get the impedance Z across the two branches as

$$Z = -\left(A_{T1}B_{T2} + B_{T1}D_{T2} + \frac{B_{T1}B_{T2}}{Z_0}\right) = Z_r + jZ_i. \quad (19)$$

Thus, we then proceed to get the expression of Z_r and Z_i. From (12), (13) and common relations of trigonometric functions, we get

$$\tan(\beta l) = \begin{cases} p, & \text{at } f_1 \\ -p, & \text{at } f_2 \end{cases} \quad (20)$$

$$\sin(\beta l) = \begin{cases} \dfrac{2p}{1+p^2}, & \text{at } f_1 \\ -\dfrac{2p}{1+p^2}, & \text{at } f_2 \end{cases} \quad (21)$$

$$\cos^2(\beta l) = \frac{1}{1+p^2}, \qquad \sin^2(\beta l) = \frac{p^2}{1+p^2}. \quad (22)$$

Rewriting (19) via (15), (16) and (20)–(22), and after some manipulations, the real and the imaginary part of Z can be obtained

as

$$Z_r = \frac{Z_0 p^2}{\left(1+p^2\right)^2 k^2}\left[\frac{2k\left(k^2+1\right)^2 p^2}{H} + 2k\left(k^2+1\right) + \frac{kH}{2p^2}\right],$$
$$Z_i = \begin{cases} X & \text{at } f_1 \\ -X & \text{at } f_2 \end{cases}, \tag{23}$$

where

$$X = \frac{Z_0 p\left(H - 2\left(k^2+1\right)\right)}{2k^2\left(1+p^2\right)^2}\left[\left(k^2+1\right)\sqrt{\frac{2p^2 k}{H}} + \sqrt{\frac{kH}{2p^2}}\right]. \tag{24}$$

And, to determine the sign of X, it is very useful to obtain the following equivalent deformation equation,

$$H-2(k^2+1)=\sqrt{(k^2+k+1)^2+4(p^4-1)k(k^2+1)}-(k^2+k+1). \tag{25}$$

According to (23), the imaginary part of isolation parameter Z will change the sign only when the frequency changes from f_1 to f_2 while the real part remains constant. Another thing worthy of note is that (23) also holds its validity in the case when the voltage source is linked to port 3 by considering the symmetry of the transmission matrices, namely $(Z_1, Z_2, Z_3, Z_4) \Rightarrow (Z_3, Z_4, Z_1, Z_2)$. In addition, based on (23) and (24), the parameters of the isolation structure Z in terms of impedances and admittances at the two desired frequencies can be respectively expressed as

$$Y(f_1) = \frac{Z_r - jX}{Z_r^2 + X^2}, \quad Y(f_2) = \frac{Z_r + jX}{Z_r^2 + X^2}. \tag{26a}$$
$$Z(f_1) = Z_r + jX, \quad Z(f_2) = Z_r - jX. \tag{26b}$$

In the following subsection, the physical implementations of the isolation structure will be discussed according to the value of X.

2.3. Lumped Components for Isolation Structure Design

In practical circuit, the two structures illustrated respectively in Figure 3 and Figure 4 can be used to implement the isolation structure Z.

The sign of X is of crucial importance, because it determines the choice of the isolator's structure among parallel RLC, series RLC and just resistor. From (13), we find $p > 0$, so the sign of X is exclusively determined by the value of expression (25). By discussing the sign of X, we will design the parameters of the isolator of parallel RLC, series RLC and resistor, respectively, in the following subsections.

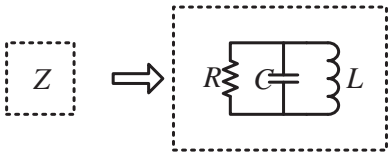

Figure 3. Isolator realized by parallel RLC circuit.

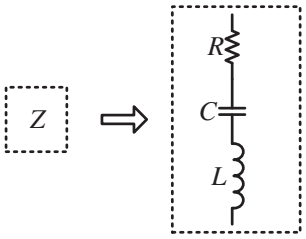

Figure 4. Isolator realized by series RLC circuit.

2.3.1. Lumped Parameters Design for Figure 3

From (25), In order to make $X > 0$, the following situation can be given by

$$p^4 > 1. \tag{27}$$

From (13), the corresponding u should satisfy

$$1 \leq u < 3. \tag{28}$$

In this case, we should choose the structure in Figure 3 as the isolation structure. Considering the parallel structure in Figure 3 and the simplicity in expression, the admittance form is employed, that is

$$\begin{aligned} Y(f_1) &= \frac{1}{R} + j2\pi f_1 C - j/(2\pi f_1 L), \\ Y(f_2) &= \frac{1}{R} + j2\pi f_2 C - j/(2\pi f_2 L). \end{aligned} \tag{29}$$

Equatons (26a) to (29), the parameters of lumped components can be obtained as follows,

$$R = \frac{Z_r^2 + X^2}{Z_r} = \frac{1 + k^2}{k} Z_0, \tag{30}$$

$$C = \frac{X}{2\pi(Z_r^2 + X^2)} \frac{1}{(f_2 - f_1)} = \frac{X}{2\pi(Z_r^2 + X^2) f_1 (u - 1)}, \tag{31}$$

$$L = \frac{\frac{f_2}{f_1} - \frac{f_1}{f_2}}{\frac{2\pi X}{Z_r^2 + X^2}(f_1 + f_2)} = \frac{(u - 1)(Z_r^2 + X^2)}{2\pi u X f_1}. \tag{32}$$

2.3.2. Lumped Parameters Design for Figure 4

Similarly, in order to satisfy $X < 0$, the following situation should be,

$$p^4 < 1. \tag{33}$$

The according u satisfies as follows,

$$u > 3. \tag{34}$$

In this case, the structure of Figure 4 needs to be chosen. Considering that the structure is series, the impedance is applied and the corresponding values are the following,

$$\begin{aligned} Z(f_1) &= R + j2\pi f_1 L - j/(2\pi f_1 C), \\ Z(f_2) &= R + j2\pi f_2 L - j/(2\pi f_2 C). \end{aligned} \tag{35}$$

Equations (26b) to (35), the parameters of lumped components can be obtained as follows,

$$R = Z_r, \tag{36}$$

$$C = \frac{\frac{f_2}{f_1} - \frac{f_1}{f_2}}{-2\pi X(f_1 + f_2)} = \frac{u-1}{-2\pi u X f_1}, \tag{37}$$

$$L = \frac{-X}{2\pi(f_2 - f_1)} = \frac{-X}{2\pi f_1(u-1)}. \tag{38}$$

2.3.3. Resistance Design without Reactive Components

From the above discussion, it can be found that $X = 0$ and $p = 1$ is the special case when $u = 3$. In this case the reactive components should be removed, and the structure of isolation will simplify to a single resistor R with the resistance value

$$R = \frac{Z_r^2 + X^2}{Z_r} = Z_r = \frac{1 + k^2}{k} Z_0. \tag{39}$$

Obviously, this is the same with the conventional unequal Wilkinson power divider using 1/4 wavelength transmission lines [8], and this means the conventional unequal divider is just a special case of our proposed power divider.

In summary, parameters of this unequal dual-frequency Wilkinson power divider can be calculated directly by (5)–(9), (13) and (30)–(32) or (36)–(38) or (39) according to different desired frequency ratio u. Especially for the special case of equal Wilkinson power divider when $k = 1$, the circuit parameters can be obtained from (7), (8), (30)–(32), i.e., $R = 2Z_0$ and $Z_i = Z_0$, $i = 5, 6, 7, 8$, which is in accordance with the results discussed in [13].

2.4. Analysis of Available Frequency-ratio Range

Using the analytical design Equations (5)–(9) and (13), we can obtain the available ranges of frequency ratios for different power dividing ratios when constraining the source impedance $Z_0 = 50\,\Omega$ and all the impedances in the practical range of $35\ \Omega \sim 140\,\Omega$. Several samples are given below

$$u = \begin{cases} 1 \sim 8, & k = 1; \\ 1 \sim 7.1, & k = 1.1; \\ 1 \sim 6.4, & k = 1.2; \\ 1 \sim 5.7, & k = 1.3; \\ 1 \sim 5, & k = \sqrt{2}; \\ 1 \sim 4.5, & k = 1.5. \end{cases} \tag{40}$$

From (40), wide available frequency-ratio ranges can be observed. It is even notable that the available frequency-ratio ranges can remain quite wide in the unequal power division cases, and it is especially useful in the microwave engineering.

3. SIMULATIONS AND EXPERIMENTS

To certify the unequal division and effective isolation at two arbitrary frequencies, simulations and experiments on two examples of unequal dual-frequency power dividers are presented. The first example includes the parallel RLC isolator while the second example includes the series RLC isolator. It is necessary to point out that these simulations are based on ideal transmission line and circuit models (closed-form equation models) and the power dividers are designed without any optimization methods and EM simulation. In these experiments, the S parameters of two power dividers are measured by Agilent E5071C network analyzer (maximum test frequency 4.5 GHz). With port impedance $Z_0 = 50\,\Omega$ and power dividing ratio $k = \sqrt{2}$, two unequal dual-frequency Wilkinson power dividers have been designed and fabricated as follows.

Figure 5. The fabricated unequal dual-frequency Wilkinson power divider in the first example.

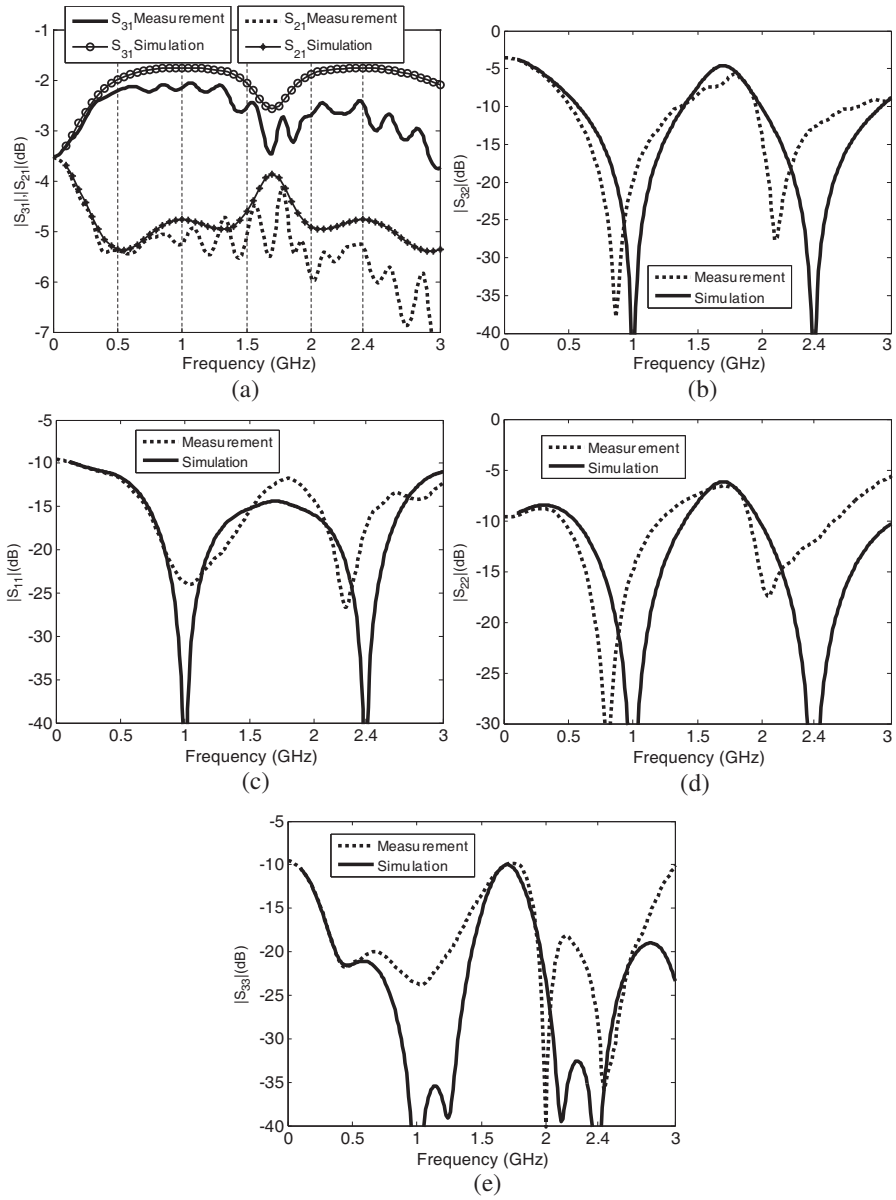

Figure 6. The simulation and measurement results of the first example: (a) Magnitude of S_{31} and S_{21}. (b) Magnitude of S_{32}. (c) Magnitude of S_{11}. (d) Magnitude of S_{22}. (e) Magnitude of S_{33}.

3.1. The First Example: Power Divider with Parallel RLC Isolator

In the first example, the unequal power divider is expected to operate at two center frequencies $f_1 = 1\,\text{GHz}$ and $f_2 = 2.4\,\text{GHz}$ (This case cannot be designed by the mathematical design equations in [23]). The design parameters of this unequal dual-frequency divider should be first calculated. The frequency ratio $u = 2.4 < 3$, thus, according to the discussion in Section 2, the parallel RLC isolation circuit shown in Figure 3 should be chosen. Then based on (5)–(9), (12), (13), (23), (24) and (30)–(32), the design parameters can be obtained directly: $X = 26.90 > 0$, $l = 0.1471\lambda_1$, $R = 106.07\,\Omega$, $C = 0.29\,\text{pF}$, $L = 36.15\,\text{nH}$, $Z_1 = 111.47\,\Omega$, $Z_2 = 95.155\,\Omega$, $Z_3 = 55.733\,\Omega$, $Z_4 = 47.577\,\Omega$, $Z_5 = 61.706\,\Omega$, $Z_6 = 57.297\,\Omega$, $Z_7 = 40.515\,\Omega$, $Z_8 = 43.633\,\Omega$. Practically in the experiment, this unequal dual-frequency power divider has been fabricated on a FR-4 substrate ($h = 0.8\,\text{mm}$, $\varepsilon_r = 4.6$, $\tan\delta = 0.035$), and its photograph is shown in Figure 5. Figure 6 gives the simulation and measurement results of S parameters. The simulation results show the good performance of the designed power divider, including effective input matching, output isolation, and power dividing ratios close to theoretical values at both f_1 and f_2. In measurement results, the following details are obtained: (i) the values of $|S_{21}|$ are $-5.24\,\text{dB}$ at 1 GHz and $-5.3\,\text{dB}$ at 2.4 GHz, while the values of $|S_{31}|$ are $-2.15\,\text{dB}$ at 1 GHz and $-2.46\,\text{dB}$ at 2.4 GHz. Thus the measured power dividing ratios are $-2.15-(-5.24) = 3.09\,\text{dB}$ at 1 GHz and $-2.46-(-5.3) = 2.84\,\text{dB}$ at 2.4 GHz, both of which are very close to the theoretical designed unequal power dividing ratio of 3 dB. (ii) $|S_{32}|$ reflects the isolation between Port 2 and Port 3. Figure 6(b) illustrates that the values of $|S_{32}|$ at both center frequencies are below $-12\,\text{dB}$, and this shows the good isolation effect of the parallel RLC isolator. (iii) $|S_{11}|$ reflects the degree of input matching. Figure 6(c) shows the input matching parameters (i.e., $|S_{11}|$) are below $-17\,\text{dB}$ at both f_1 and f_2. This means an effective input matching at Port 1. Similarly, the output matching parameters (i.e., $|S_{22}|$ and $|S_{33}|$) are below $-12\,\text{dB}$ at both 1 GHz and 2.4 GHz.

3.2. The Second Example: Power Divider with Series RLC Isolator

In this example, different from the first example, $f_1 = 1\,\text{GHz}$ and $f_2 = 4\,\text{GHz}$ are considered. In this case, the frequency ratio $u = 4 > 3$, thus, according to the discussion in Section 2, the series RLC isolation circuit shown in Figure 4 is chosen. Then based on (5)–(9), (13), (23), (24) and (36)–(38), the following parameters can be also obtained:

$X = -27.92 < 0$, $R = 98.12$, $C = 4.27\,\text{pF}$, $L = 1.48\,\text{nH}$, $Z_1 = 88.62\,\Omega$, $Z_2 = 119.68\,\Omega$, $Z_3 = 44.31\,\Omega$, $Z_4 = 59.84\,\Omega$, $Z_5 = 55.14\,\Omega$, $Z_6 = 64.12\,\Omega$, $Z_7 = 45.34\,\Omega$, $Z_8 = 38.99\,\Omega$. Considering that $f_2 = 4\,\text{GHz}$ in this example is higher than the $f_2 = 2.4\,\text{GHz}$ in the first example and that the frequency characteristics of FR-4 are prone to distort easily in high frequency range, it is necessary to apply another kind of substrate to avoid possible high frequency distortions. Thus, the second unequal dual-frequency power divider has been fabricated on a F4B substrate ($h = 0.8\,\text{mm}$, $\varepsilon_r = 2.65, \tan\delta = 0.001$). The photograph of fabricated power divider is shown in Figure 7 and the simulation and measurement results of S parameters are presented in Figure 8. In measurement results, the values of $|S_{21}|$ are $-5.11\,\text{dB}$ at 1 GHz and $-6.37\,\text{dB}$ at 4 GHz, while the values of $|S_{31}|$ are $-1.73\,\text{dB}$ at 1 GHz and $-1.97\,\text{dB}$ at 4 GHz. Therefore, the power dividing ratios are 3.38 dB at 1 GHz and 4.4 dB at 4 GHz. The isolation parameters (i.e., $|S_{32}|$) and input matching parameters (i.e., $|S_{11}|$) are all below $-15\,\text{dB}$ at both 1 GHz and 4 GHz, and the output matching parameters (i.e., $|S_{22}|$ and $|S_{33}|$) are below $-20\,\text{dB}$ at both 1 GHz and 4 GHz.

3.3. Results Analysis

Simulation and experiment results show that our proposed unequal dual-frequency Wilkinson power divider performs well and the design method are applicable. The power dividing ratio is close to theoretical designed value, the frequency ratio varies in a wide range and a good isolation effect at dual-frequency can be obtained using the proposed isolator in different frequency-ratio cases. In addition, it can be observed from the simulation results that the operating bandwidth is up to 200 MHz at each frequency when the parameters of isolation and matching are all below $-20\,\text{dB}$. And this means the proposed power divider can be used in many kinds of dual band wireless systems with

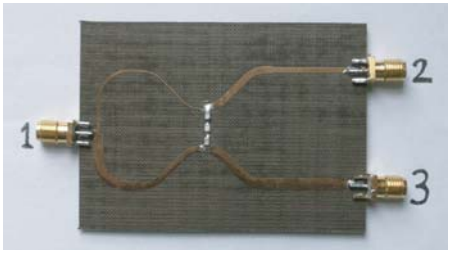

Figure 7. The fabricated unequal dual-frequency Wilkinson power divider in the second example.

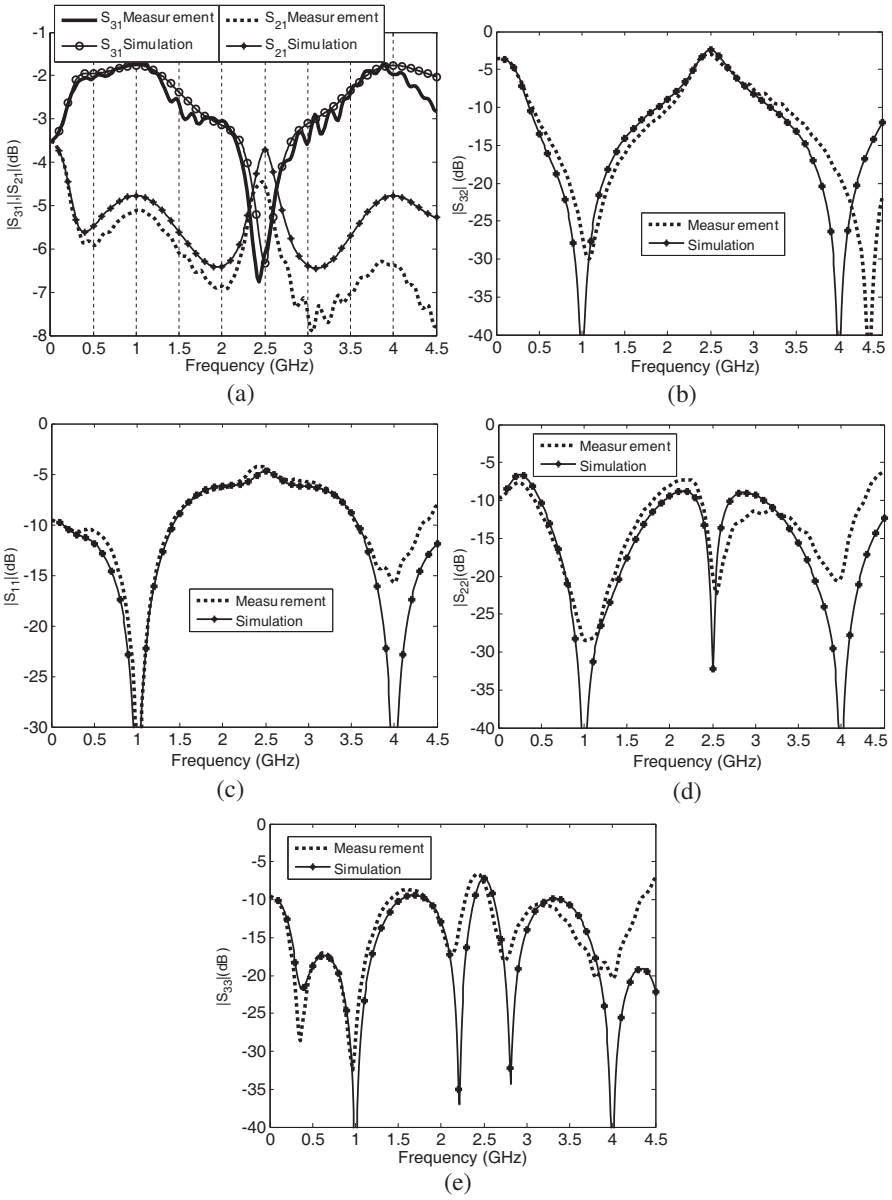

Figure 8. The simulation and measurement results of the second example: (a) Magnitude of S_{31} and S_{21}. (b) Magnitude of S_{32}. (c) Magnitude of S_{11}. (d) Magnitude of S_{22}. (e) Magnitude of S_{33}.

wide bandwidth.

However, there are also some slight differences between experiment and simulation. In the experiment results, we find some frequency offset and magnitude loss when comparing with the simulation results and they increase as the frequency increases. This also shows the existence of influence of high frequency. The values of power dividing ratios are not so close to the theoretical value of 3 dB in the second example. Judging from the results, we think that these disagreements should be caused by the following factors we did not take into consideration in this paper: (i) Losses and high frequency characteristic distortions of the substrates (especially FR4) are ignored in the theoretical design process, and the parameters of the lumped components would deviate from the nominal value at high frequency (e.g., 4 GHz in the second example). (ii) The interference of EM transmission caused by the junction discontinuities is also not considered in the design process. (iii) Fabrication tolerance and connectors (SMA) losses are included in these experiments. Although further consideration of these factors may improve the precision of our design model, our simple method has already provided general information and useful guidance for generalized unequal dual-frequency power divider design.

In summary, judging from the preceding discussions, the performance of the two fabricated unequal dual-frequency Wilkinson power dividers can fulfill our design goal, and this can also certify the validity of the proposed structures and the final closed-form design methods.

4. CONCLUSION

The theoretical closed-form design method and practical implementation of a generalized unequal arbitrary dual-frequency Wilkinson power divider have been proposed in this paper. A comprehensive analytical design scheme is given by several mathematical expressions in the design section. Then, the analytical design process is verified by experiments including two examples with different isolation structures. From the analysis results, the wide available frequency-ratio range and the flexible choice of isolation structure accordingly are main advantages of this unequal dual-frequency power divider. More importantly in theory, the proposed generalized power dividers can be regarded as a generalized model, which combines the equal dual-frequency modified Wilkinson power divider ($k = 1$) [13], the unequal Wilkinson power divider for a frequency and its first harmonic ($u = 2$) [23] and the traditional unequal single band Wilkinson power divider ($u = 3$) [8].

ACKNOWLEDGMENT

The authors want to express their gratitude to the partial financial support of National High Technology Research and Development Program of China (863 Program, No. 2008AA01Z211) and Project of Guangdong Province Education Ministry Demonstration Base of Combining Production, Teaching and Research (No. 2007B090200012). The authors would like to thank Yuewang Huang and Haiyu Huang (at Department of Electrical Engineering, Columbia University) for revising this paper.

APPENDIX A.

Here, we present the deduction of Equations (30) and (39). To begin with, (30) is considered. From (23) and (24), we get

$$\frac{X^2}{Z_r} = \frac{Z_0[H-2(k^2+1)]^2}{4k^2(1+p^2)^2}, \tag{A1}$$

Thus

$$R = Z_r + \frac{X^2}{Z_r} = Z_0 \frac{p^2}{(1+p^2)^2k^2} \times \left[\frac{2k(k^2+1)^2p^2}{H} + 2k(k^2+1) + \frac{kH}{2p^2} + \frac{[H-2(k^2+1)]^2}{4p^2}\right]. \tag{A2}$$

From (9), we can obtain the following equation,

$$\frac{1}{H} = \frac{\left[k-k^2-1+\sqrt{(k-k^2-1)^2+4p^4k(k^2+1)}\right]}{4p^4k(k^2+1)}. \tag{A3}$$

Substituting (9) and (A3) to (A2), the value of R can be given by

$$\begin{aligned} R = Z_0 \frac{1}{4(1+p^2)^2k^2} \times \big[&2\left(k^2+1-k\right)\left(k-k^2-1\right) \\ &+2(k^2+1+k)\sqrt{(k-k^2-1)^2+4p^4k(k^2+1)} \\ &+8k(k^2+1)p^2+\left[\sqrt{(k-k^2-1)^2+4p^4k\,(k^2+1)}-\left(k+k^2+1\right)\right]^2\Big]. \end{aligned} \tag{A4}$$

Then (A4) can be rewritten as,

$$\begin{aligned} R = Z_0 \frac{1}{4(1+p^2)^2k^2} \times \big[&(k^2+1-k)(k-k^2-1) \\ &+8k(k^2+1)p^2+4p^4k(k^2+1)+(k+k^2+1)^2\big]. \end{aligned} \tag{A5}$$

And for further simplification, (A5) can be expressed as,

$$R = Z_0 \frac{4k(k^2+1)}{4(1+p^2)^2k^2} \times \left[1 + 2p^2 + p^4\right]. \tag{A6}$$

Finally, from (A6) we can obtain the final design equation,

$$R = \frac{k^2+1}{k} Z_0. \tag{A7}$$

Then, we consider (39), which is given by

$$Z_r|_{\,p=1} = \frac{Z_0}{4k^2}[k(k^2+1) + 2k(k^2+1) + k(k^2+1)] = \frac{(k^2+1)}{k} Z_0. \tag{A8}$$

Therefore, (30) and (39) have been proved mathematically.

REFERENCES

1. Shynu, S. V., G. Augustin, C. K. Aanandan, P. Mohanan, and K. Vasudevan, "Design of compact reconfigurable dual frequency microstrip antennas using varactor diodes," *Progress In Electromagnetics Research*, PIER 60, 197–205, 2006.
2. Zainud-Deen, S. H., S. M. Gaber, and S. M. M. Ibrahem, "Built-in dual frequency antenna with an embedded camera and a vertical ground plane," *Progress In Electromagnetics Research Letters*, Vol. 3, 51–60, 2008.
3. He, Z., X.-L. Wang, S. Han, T. Lin, and Z. Liu, "The synthesis and design for new classic dual-band waveguide band-stop filters," *Journal of Electromagnetic Waves and Applications*, Vol. 22, 119–130, 2008.
4. Monzon, C., "A small dual frequency transformer in two sections," *IEEE Trans. Microw. Theory Tech.*, Vol. 51, No. 4, 1157–1161, 2003.
5. Wu, Y., Y. Liu, and S. Li, "A compact Pi-structure dual band transformer," *Progress In Electromagnetics Research*, PIER 88, 121–134, 2008.
6. Castaldi, G., V. Fiumara, and I. Gallina, "An exact synthesis method for dual-band chebyshev impedance transformers," *Progress In Electromagnetics Research*, PIER 86, 305–319, 2008.
7. Wu, Y., Y. Liu, and S. Li, "A dual-frequency transformer for complex impedances with two unequal sections," *IEEE Microw. Wireless Compon. Lett.*, Vol. 19, No. 2, 77–79, 2009.

8. Wilkinson, E., "An N-way hybrid power divider," *IRE Trans. Microw. Theory Tech.*, Vol. 8, No. 1, 116–118, 1960.
9. Chen, H. and Y. Zhang, "A novel compact planar six-way power divider using folded and hybrid-expanded coupled lines," *Progress In Electromagnetics Research*, PIER 76, 243–252, 2007.
10. Ruiz-Cruz, J. A., J. R. Montejo-Garai, J. M. Rebollar, and S. Sobrino, "Compact full Ku-band triplexer with improved E-plane power divider," *Progress In Electromagnetics Research*, PIER 86, 39–51, 2008.
11. Wu, Y. and Y. Liu, "Closed-form design method for unequal lumped-elements wilkinson power dividers," *Microwave and Optical Technology Letters*, Vol. 51, No. 5, 1320–1324, 2009.
12. Srisathit, S., M. Chongcheawchamnan, and A. Worapishet, "Design and realisation of dual-band 3 dB power divider based on two-section transmission-line topology," *Electronics Letters*, Vol. 39, No. 9, 723–724, 2003.
13. Wu, L., Z. Sun, H. Yilmaz, and M. Berroth, "A dual-frequency Wilkinson power divider," *IEEE Trans. Microw. Theory Tech.*, Vol. 54, No. 1, 278–284, 2006.
14. Kawai, T., Y. Nakashima, Y. Kokubo, and I. Ohta, "Dual-band Wilkinson power dividers using a series RLC circuit," *IEICE Trans. Electron.*, Vol. E91-C, No. 11, 1793–1797, 2008.
15. Wu, Y., Y. Liu, and S. Li, "A new dual-frequency Wilkinson power divider," *Journal of Electromagnetic Waves and Applications*, Vol. 23, 483–492, 2009.
16. Cheng, K.-K. M. and F.-L. Wong, "A new Wilkinson power divider design for dual band application," *IEEE Microw. Wireless Compon. Lett.*, Vol.17, No. 9, 664–666, 2007.
17. Cheng, K.-K. M. and C. Law, "A novel approach to the design and implementation of dual-band power divider," *IEEE Trans. Microw. Theory Tech.*, Vol. 56, No. 2, 487–492, 2008.
18. Park, M.-J. and B. Lee, "A dual-band Wilkinson power divider," *IEEE Microw. Wireless Compon. Lett.*, Vol. 18, No. 2, 85–87, 2008.
19. Park, M.-J. and B. Lee, "Wilkinson power divider with extended ports for dual-band operation," *Electronics Letters*, Vol. 44, No. 15, 916–917, 2008.
20. Wu, Y., Y. Liu, and X. Liu, "Dual-frequency power divider with isolation stubs," *Electronics Letters*, Vol. 44, No. 24, 1407–1408, 2008.
21. Kampitaki, D. G., A. T. Hatzigaidas, A. I. Papastergiou, and

Z. D. Zaharis, "On the design of a dual-band unequal power divider useful for mobile communications," *Electrical Engineering*, Vol. 89, No. 6, 443–450, 2007.

22. Feng, C., G. Zhao, X. F. Liu, and F. S. Zhang, "A novel dual-frequency unequal wilkinson power divider," *Microwave and Optical Technology Letters*, Vol. 50, No. 6, 1695–1699, 2008.
23. Wu, Y., H. Zhou, Y. Zhang, and Y. Liu, "An unequal Wilkinson power divider for a frequency and its first harmonic," *IEEE Microw. Wireless Compon. Lett.*, Vol. 18, No. 11, 737–739, 2008.
24. Wu, Y., Y. Liu, Y. Zhang, J. Gao, and H. Zhou, "A dual band unequal wilkinson power divider without reactive components," *IEEE Trans. Microw. Theory Tech.*, Vol. 57, No. 1, 216–222, 2009.
25. Wu, Y., Y. Liu, and S. Li, "Unequal dual-frequency Wilkinson power divider including aeries resistor-inductor-capacitor isolation structure," *IET Microwaves, Antennas & Propagation*, Vol. 3, in press, 2009.
26. Wu, Y., Y. Liu, and S. Li, "A novel design method for unequal dual-frequency Wilkinson power divider," submitted to *Microwave and Optical Technology Letters*, 2009.
27. Wu, Y., Y. Liu, and S. Li, "A compact unequal Wilkinson power divider for dual-frequency applications," submitted to *Microwave and Optical Technology Letters*, 2009.